Journal of Magnetic Resonance 312 (2020) 106688

Contents lists available at ScienceDirect

Journal of Magnetic Resonance

journal homepage: www.elsevier.com/locate/jmr

Heteronuclear cross-relaxation effect modulated by the dynamics of N-functional groups in the solid state under ^{15}N DP-MAS DNP

Heeyong Park [a,b,e], Boran Uluca-Yazgi [c,f], Saskia Heumann [a], Robert Schlögl [a,d], Josef Granwehr [b,e], Henrike Heise [c,f], P. Philipp M. Schleker [a,b,*]

[a] Max Planck Institute for Chemical Energy Conversion, Department of Heterogeneous Reactions, 45470 Mülheim an der Ruhr, Germany
[b] Forschungszentrum Jülich, IEK-9, 52425 Jülich, Germany
[c] Forschungszentrum Jülich, IBI-7 and JuStruct, 52425 Jülich, Germany
[d] Fritz Haber Institute of the Max Planck Society, 14195 Berlin, Germany
[e] RWTH Aachen University, Institute of Technical and Macromolecular Chemistry, 52074 Aachen, Germany
[f] Heinrich Heine Universität Düsseldorf, Institute of Physical Biology, 40225 Düsseldorf, Germany

ARTICLE INFO

Article history:
Received 27 November 2019
Revised 12 January 2020
Accepted 14 January 2020
Available online 16 January 2020

Keywords:
Cross-relaxation
DNP
NMR
Dynamics
N-functional group
DNP-SENS
SCREAM
CRE
NOE

ABSTRACT

In a typical magic-angle spinning (MAS) dynamic nuclear polarization (DNP) nuclear magnetic resonance (NMR) experiment, several mechanisms are simultaneously involved when transferring much larger polarization of electron spins to NMR active nuclei of interest. Recently, specific cross-relaxation enhancement by active motions under DNP (SCREAM-DNP) [Daube et al. JACS 2016] has been reported as one of these mechanisms. Thereby ^{13}C enhancement with inverted sign was observed in a direct polarization (DP) MAS DNP experiment, caused by reorientation dynamics of methyl that was not frozen out at 100 K. Here, we report on the spontaneous polarization transfer from hyperpolarized ^{1}H to both primary amine and ammonium nitrogens, resulting in an additional positive signal enhancement in the ^{15}N NMR spectra during ^{15}N DP-MAS DNP. The cross-relaxation induced signal enhancement (CRE) for ^{15}N is of opposite sign compared to that observed for ^{13}C due to the negative sign of the gyromagnetic ratio of ^{15}N. The influence on CRE efficiency caused by variation of the radical solution composition and by temperature was also investigated.

1. Introduction

Dynamic Nuclear Polarization (DNP) is an emerging magnetic resonance technique to enhance the sensitivity of high-field magic-angle spinning (MAS) nuclear magnetic resonance (NMR) [1–4]. DNP enables signal enhancement, defined as the spin polarization achieved by DNP relative to the thermal equilibrium polarization of the respective nucleus, up to several orders of magnitude by transferring the large electron-spin polarization of paramagnetic polarizing agents to target NMR nuclei using microwave (MW) irradiation at specific frequencies. Alleviating the low sensitivity, which is the key challenge of traditional NMR spectroscopy, DNP has been successfully applied not only to the study of various biological samples [5–7] but also to solid samples in materials science [8–14]. However, despite substantial advances in DNP methodology [15,16] and instrumentation [17–19], NMR sensitivity is still a limiting factor in many applications [3]. Therefore, it is important to understand the different polarization transfer mechanisms occurring simultaneously during DNP in order to enable a systematic optimization of these experiments.

Molecular dynamics affecting the longitudinal relaxation time constant, T_1, which play a key role in the polarization transfer processes, are often neglected in MAS DNP measurements that are performed typically at 100 K, because most motional modes are effectively frozen out. However, some exceptional dynamics with small activation energies [20], such as the fast rotational motion of the methyl group [21], may show fast dynamical properties even at cryogenic temperatures. Recently, it has been reported that methyl group reorientation dynamics under DNP conditions can cause heteronuclear cross-relaxation mediated polarization transfer in the solid state [21–24]. Thereby, mobile methyl protons are hyperpolarized by DNP (Fig. 1(a) and (b), pink arrow). Their magnetization is then spontaneously transferred to dipolarly coupled carbon atoms by cross-relaxation (Fig. 1(a) and (b), red arrow), resulting in a negatively enhanced ^{13}C resonance signal in a direct

* Corresponding author at: Forschungszentrum Jülich, IEK-9, 52425 Jülich, Germany.
E-mail address: philipp.schleker@cec.mpg.de (P. Philipp M. Schleker).

https://doi.org/10.1016/j.jmr.2020.106688
1090-7807/

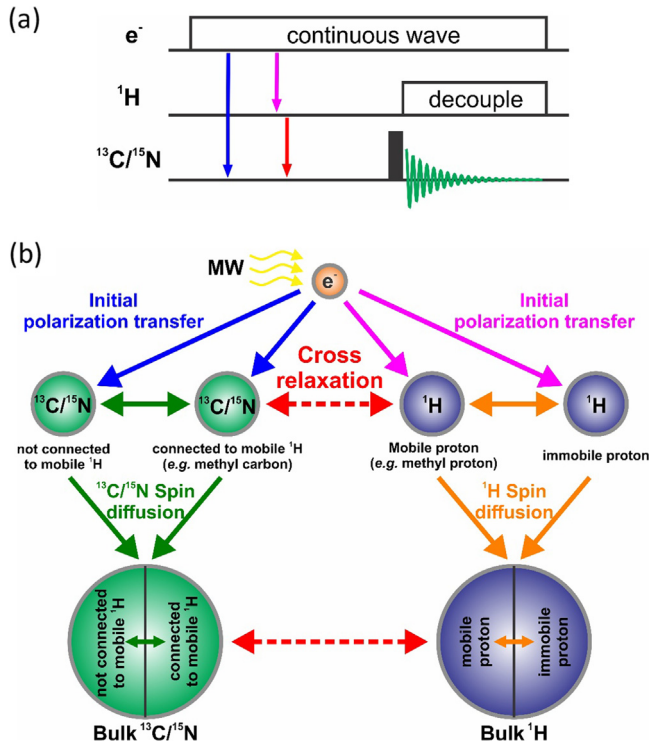

Fig. 1. (a) $^{13}C/^{15}N$ DP-MAS DNP NMR pulse sequence, and (b) the process of polarization transfer during DP-MAS DNP. Pink and blue arrow: initial hyperpolarization of ^{1}H and $^{13}C/^{15}N$ by DNP. Red arrow: spontaneous polarization transfer (cross-relaxation) from hyperpolarized ^{1}H to $^{13}C/^{15}N$ connected to mobile ^{1}H. Green and orange arrow: polarization transfer to other $^{13}C/^{15}N$ and ^{1}H by homonuclear spin diffusion [27,28]. (For interpretation of the references to colour in this figure legend, the reader is referred to the web version of this article.)

polarization (DP) MAS NMR experiment. The transferred polarization subsequently spreads to other carbons through the ^{13}C dipolar network by ^{13}C-^{13}C spin diffusion (Fig. 1(b), green arrow). This cross-relaxation process is identical to that underlying the Nuclear Overhauser Effect (NOE) [25]: saturation of proton spins with on-resonance radio frequency (rf) pulses results in a positive signal enhancement in the ^{13}C NMR spectra even in solids if the dynamics occur on a favorable time scale [26]. Under DNP conditions, when proton spins are hyperpolarized instead of saturated, double quantum cross-relaxation between ^{1}H and ^{13}C spins results in a negative signal enhancement, which is opposite in sign to typical NOE enhancement in ^{13}C NMR.

Up to now, the cross-relaxation effect in DP-MAS DNP NMR has only been reported for ^{13}C nuclei. Here, it is investigated whether such an effect can also be confirmed for ^{15}N by providing experimental evidence for cross-relaxation mediated enhancement (CRE) during ^{15}N DP-MAS DNP using benzyl ammonium and glutamine as model compounds (Fig. 2).

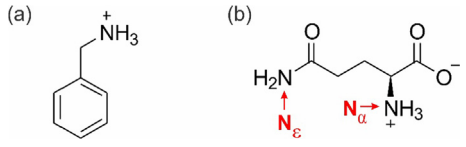

Fig. 2. Model compounds (a) benzyl ammonium and (b) glutamine as mobile primary ammonium and amine representatives. The nitrogen names (N_α and $N\varepsilon$) of glutamine are represented in the structure.

2. Theoretical background

The cross-relaxation mediated polarization transfer can be modelled by starting with the Solomon equations [22,29] for two dipole-coupled spins *I*, *S*. To empirically include solid-state DNP, the equations of motion for a closed two-spin system can be amended by a term that supplies non-equilibrium polarization from the outside. This corresponds to the coupling of the two-spin system to an external "DNP bath", with the hypothetical steady-state polarization enhancement values ε_I^0 and ε_S^0 and corresponding enhancement rates ρ_I^{DNP} and ρ_S^{DNP} for the *I* and the *S* spin, respectively (for details see electronic Supporting Information). ε_I^0 and ε_S^0 correspond to the DNP enhancement factors that would be achieved without coupling between *I* and *S* and with infinitely slow relaxation towards thermal equilibrium. For such a system, the total steady-state *S* spin polarization enhancement (ε_{tot}) including cross-relaxation under DNP is

$$\varepsilon_{tot} = 1 + \frac{\rho_S^{DNP}(\varepsilon_S^0 - 1)}{\rho_S + \rho_S^{DNP}} - (\varepsilon_I - 1)\frac{\gamma_I}{\gamma_S}\frac{\sigma_{IS}}{\rho_S + \rho_S^{DNP}} \quad (1)$$

For the systems studied here, ε_{tot} is the ^{15}N enhancement factor, or ^{15}N spin polarization relative to its thermal equilibrium, and ε_I is the actual steady-state enhancement factor of ^{1}H. γ_I and γ_S are the gyromagnetic ratios of ^{1}H and ^{15}N, respectively. σ_{IS} is the ^{1}H-^{15}N cross-relaxation rate and ρ_S is the ^{15}N longitudinal relaxation rate without coupling to the DNP bath. The first term on the right-hand side of this equation presents thermal equilibrium polarization (TP), the second term constitutes ^{15}N direct enhancement (ΔDE) achieved without the influence of cross-relaxation, and the third term represents the contribution from cross-relaxation effect (ΔCRE or ΔNOE). Notice the similarity of this third contribution with the enhancement in liquid-state Overhauser DNP, where the factor $\sigma_{IS}/(\rho_S + \rho_S^{DNP})$ has been identified as the product of a coupling factor between the two spins and a leakage factor caused by relaxation back to thermal equilibrium [30].

The equation for the polarization enhancement may be simplified if it can be assumed that the DNP enhancement rate is much higher than the spin–lattice relaxation rate, *i.e.* $\rho_S^{DNP} \gg \rho_S$, which often applies at cryogenic temperatures. Then we get

$$\varepsilon_{tot} \approx \varepsilon_S^0 - (\varepsilon_I - 1)\frac{\gamma_I}{\gamma_S}\frac{\sigma_{IS}}{\rho_S^{DNP}} \quad (2)$$

If, on the other hand, ^{15}N direct enhancement (ΔDE) on mechanisms other than cross-relaxation mediated from the *I* spin is very low, $\rho_S^{DNP} \approx 0$, then the same expression as by Daube *et al.* is obtained [22],

$$\varepsilon_{tot} \approx \varepsilon_{CR} = 1 - (\varepsilon_I - 1)\frac{\gamma_I}{\gamma_S}\frac{\sigma_{IS}}{\rho_S} \quad (3)$$

The gyromagnetic ratio of ^{15}N (negative sign; $\gamma_N = -27.116 \times 10^6$ rad·s^{-1}·T^{-1}) has an opposite sign compared to ^{13}C (positive sign; $\gamma_C = 6.7262 \times 10^7$ rad·s^{-1}·T^{-1}), so it is expected to show an opposite signal enhancement contribution in both CRE (the spontaneous Cross-Relaxation induced Enhancement under DNP) and the typical NOE. For example, if the substance of interest contains protonated nitrogen functional groups, which can rotate fast enough even at 100 K to facilitate cross-relaxation, hyperpolarization of ^{1}H ($\varepsilon_I > 1$) by DNP and the opposite signs of gyromagnetic ratios between ^{1}H (positive, $\gamma = 26.7513 \times 10^7$ rad·s^{-1}·T^{-1}) and ^{15}N would cause a net positive enhancement ($\varepsilon_{tot} > \varepsilon_S^0$) by CRE in the ^{15}N DP-MAS DNP NMR spectrum. On the other hand, saturation of ^{1}H ($\varepsilon_I = 0$) would induce a net negative enhancement ($\varepsilon_{tot} < \varepsilon_S^0$), a phenomenon that is traditionally called hetNOE [25,31].

In this paper, nomenclatures and symbols as shown in Table 1 are used to explain the spontaneous cross-relaxation induced

Table 1
Nomenclatures of observable effects depending on the experiment condition in this paper[a].

Experiment condition		Contributions to the signal intensity	Condition of ε_I	Contribution of cross-relaxation effect (ΔCRE or ΔNOE) on ^{15}N signal enhancement
Microwave	^{1}H saturation			
Off	Off	TP	$\varepsilon_I = 1$	–
Off	On	TP + ΔNOE	$\varepsilon_I = 0$	Negative
On	Off	TP + ΔDE + ΔCRE	$\varepsilon_I > 1$	Positive
On	On	TP + ΔDE + ΔNOE	$\varepsilon_I = 0$	Negative

[a] TP (thermal equilibrium polarization), ΔNOE (signal contribution by NOE), ΔDE (signal contribution by ^{15}N direct enhancement (DE) effect under DNP), ΔCRE (signal contribution by spontaneous cross-relaxation induced enhancement (CRE) effect under DNP).

enhancement (CRE) effect occurring during the DP-MAS DNP separately from the NOE. Direct hyperpolarization (DP) defines the set of effects affecting polarization of a particular nucleus under continuous MW irradiation without any rf manipulation.

3. Experimental

All chemicals were analytical grade. The ^{15}N labeled benzyl ammonium sample was prepared by mixing ^{15}N labeled benzyl amine (98 atom % ^{15}N, Sigma Aldrich) and bis(trifluoromethylsulfonyl)imide (≥95.0%, Sigma Aldrich) in a 1:3, w/w ratio in an aprotic solvent consisting of a mixture of tetrachloroethane/DMSO d_6/DMSO in a ratio of 67/30/3 vol%. As polarizaing agent, TEKPol [32] (Cortecnet) radical was added in a final concentration of 10 mM. Since the TEKPol radical is unstable in an acidic environment and at room temperature as can be seen in Fig. S1 in the supporting information, the TEKPol radical was added just before loading the sample into the MAS rotor and cooling down. The nitrogen spectrum exhibits a quartet splitting pattern in the ^{15}N solution NMR spectrum (Fig. S2) without proton decoupling, indicating that the N-functional group exists as the primary ammonium ion.

The saturated ^{15}N/^{13}C labeled glutamine (99 atom % ^{15}N, 99 atom % ^{13}C, Sigma Aldrich) samples were prepared using three different solvents with different ^{1}H concentrations: glycerol-d_8/D_2O/H_2O (60/30/10 vol%), glycerol-d_8/H_2O (60/40 vol%), glycerol/H_2O (60/40 vol%) mixture containing 10 mM AMUPol [33] (Cortecnet) radical. To confirm that the solubility of glutamine is not affected by the different ^{1}H/^{2}H isotope ratios in the solvent, the concentration of saturated glutamine in each solvent was determined by ^{1}H NMR. The concentrations of glutamine were similar with 12.7, 12.2 and 12.2 mg/ml, respectively. The samples were then transferred into 3.2 mm sapphire rotors.

DNP experiments were performed on a Bruker (Karlsruhe, Germany) wide-bore Avance III HD 600 MHz spectrometer equipped with a triple resonance TCI (^{1}H, ^{13}C, ^{15}N) cryoprobe connected to a 395 GHz gyrotron with 60 mA of beam current as a continuous microwave source. Experiments were conducted at 100 K for all samples and additionally at 140 K for the glutamine sample in glycerol/H_2O (60/40 vol%) to confirm the temperature dependence of the cross-relaxation. For all experiments, excitation 90° pulses of 6.0 and 2.8 μs duration, corresponding to an rf field strength of 42 kHz and 89 kHz, were applied for ^{15}N and ^{1}H, respectively. SPINAL-64 decoupling was applied during acquisition with a ^{1}H rf field of *ca.* 90 kHz. The number of scans was 8 at a MAS spinning frequency of 9 kHz. The pulse sequence [24] in Fig. S3 was used to identify the intimately linked the CRE effect and the NOE, depending on the presence or absence of the ^{1}H saturation pulse train. A presaturation pulse-train with 16 90° pulses separated by 3 ms was applied to both ^{1}H and ^{15}N to destroy any transverse magnetization left. All direct DP spectra were measured using a single 90° pulse excitation of ^{15}N without ^{1}H saturation pulses. For the ^{1}H saturation experiment (DP_{sat}), 180° ^{1}H saturation pulses with a pulse interval of 500 ms (Fig. S3, d21) were used to prevent further ^{1}H polarization build-up. All DP and DP_{sat} NMR experiments were performed using 6 variable polarization delays ranging from 10 s to 600 s.

4. Results and discussion

To estimate the CRE effect and the related NOE in the ^{15}N DP-MAS DNP spectrum of the benzyl ammonium cation, ^{15}N DP measurements were conducted with and without MW irradiation as well as with and without ^{1}H saturation pulse trains as a function of polarization time. Comparisons of the different data sets according to different properties are shown in Fig. 3 and Fig. S4. As can be seen in Fig. 3(a) and S4(a), the signal intensities in the spectra and the build-up curves are drastically affected by ^{1}H saturation pulse trains, which means that the CRE effect and the NOE play a significant role at 100 K. If the primary ammonium group of benzyl ammonium were not mobile at 100 K, a CRE effect and a NOE would not be expected, and the same intensity and build-up curves would be observable in Fig. 3(a,b) and S4(a,b), regardless if a ^{1}H saturation pulse was applied or not. Likewise, ^{1}H saturation also leads to a reduction of the signal intensity in the absence of DNP hyperpolarization, as shown in Fig. 3(b) and S4(b), which is a reflection of the NOE in the ^{15}N spectrum. Comparing the effects observed in Fig. 3(a) and (b), the CRE effect contributes more strongly to the signal intensity of the ^{15}N spectrum than the NOE and the DE in this sample. From Fig. 3(c) and (d), we can determine the contribution of the CRE in the ^{15}N direct hyperpolarization effect (DP). Fig. 3(c) shows a larger difference than Fig. 3(d), which means that the CRE effect dominates the positive enhancement of the ^{15}N signal in ^{15}N DP-MAS DNP.

The full observable ^{15}N signal enhancement factor (ε_{tot}) in benzyl ammonium is strongly influenced by two different effects, the CRE (Fig. 1 a and b, red arrows), and the ^{15}N DE (Fig. 1 a and b, blue and green arrows). The ^{15}N MAS NMR spectrum recorded with ^{1}H saturation and without MW, *i.e.* without any DNP effect, shows the smallest signal intensity due to the presence of the NOE which contributes a negative signal enhancement, while the highest signal intensity is found when both the ^{15}N DE and the CRE effect contribute, which is achieved without ^{1}H saturation and with MW irradiation (Figs 3, 4 and S4). From these results, it can be seen that ammonium ion rotational mobility, which enables CRE in ^{15}N DP-MAS DNP NMR, contributes significantly to the overall ^{15}N polarization even at 100 K (Fig. 4, orange dashed line). As opposed to ^{13}C, due to the negative sign of the ^{15}N gyromagnetic ratio, an additional positive enhancement is found for the ^{15}N polarization.

To determine the CRE effect in ^{15}N DP-MAS DNP NMR spectra in a protic solvent, glutamine having one ammonium and one amide group (N_α and N_ε) with well-separated chemical shifts was used in a popular protic radical solution with a protonation degree of ~10% *i.e.*, glycerol-d_8/D_2O/H_2O (60/30/10 vol%) [34]. As seen in Fig. 5(a), 1H saturation has no impact on the signal intensity, which means the CRE effect and the NOE found in the previous benzyl ammo-

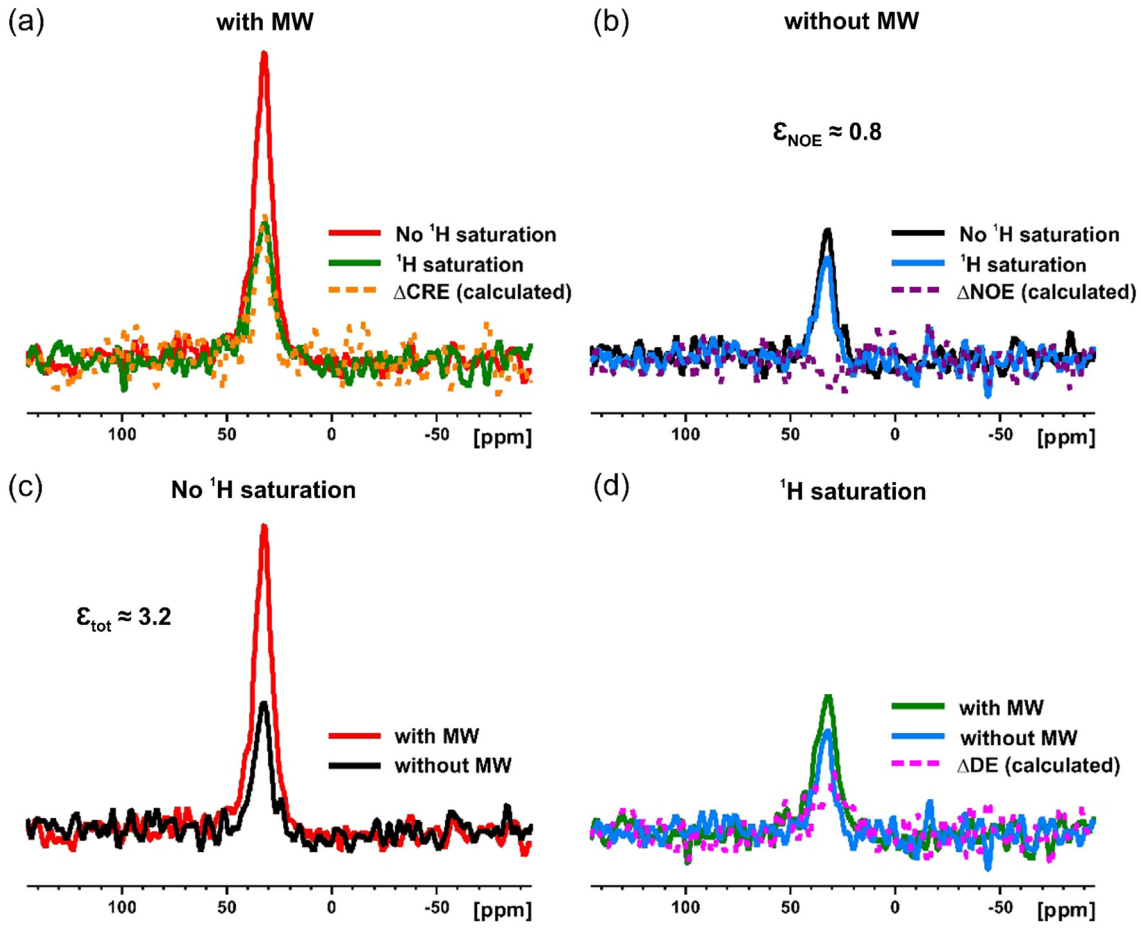

Fig. 3. ^{15}N MAS spectra of benzyl ammonium recorded after a polarization time of 600 s in the presence and absence of MW irradiation as well as ^{1}H saturation pulse trains. (a–d) Comparison of spectra (a) obtained with and without ^{1}H saturation pulses in the presence of MW irradiation, (b) obtained with and without ^{1}H saturation pulses in the absence of MW irradiation, (c) depending on the irradiation of MW without ^{1}H saturation, (d) depending on the irradiation of MW with ^{1}H saturation. For each spectrum different effects contribute to the ^{15}N NMR signal enhancement. Red: TP + ΔDE + ΔCRE, Green: TP + ΔDE + ΔNOE, Black: TP, Blue: TP + ΔNOE, Orange: ΔCRE calculated by (red-(green-(blue-black))), Purple: ΔNOE calculated by (blue-black), Pink: ΔDE calculated by (green-Blue). The dashed spectra are shown in detail in Fig. S4. (For interpretation of the references to colour in this figure legend, the reader is referred to the web version of this article.)

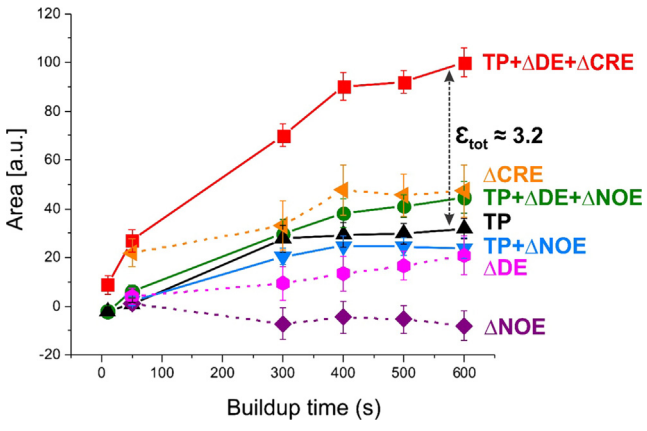

Fig. 4. Comparison plot between the four build-up curves of Fig. S4. Red: TP + ΔDE + ΔCRE *via* with MW and without ^{1}H saturation, Green: TP + ΔDE + ΔNOE *via* with MW and with ^{1}H saturation, Black: TP *via* without MW and without ^{1}H saturation, Blue: TP + ΔNOE *via* without MW and with ^{1}H saturation. The ^{15}N signal contributions of ΔCRE, ΔNOE and ΔDE were calculated from the area values of each spectrum in the same way as in Fig. 3. Orange: ΔCRE, Purple: ΔNOE, Pink: ΔDE. (For interpretation of the references to colour in this figure legend, the reader is referred to the web version of this article.)

nium sample are not significant in glutamine with this radical solution composition. This could be caused by two reasons: Either, the ^{1}H–^{15}N CRE effect induced by mobile protons under DNP conditions may be reduced because H/D exchange is expected for amine protons in protic solvent containing deuterium on the one hand (Figs. S5 and S6). Further, the amine dynamics of glutamine at 100 K could be insufficient for double quantum cross-relaxation between ^{1}H and ^{15}N on the other hand. In order to investigate this, the experiments were repeated with increasing ^{1}H concentration in the radical solution. As shown in Fig. 5(a–c), an increasing signal intensity ratio (SIR) between the data with and without proton saturation can be identified at higher ^{1}H concentration. This indicates that the protonation ratio of the amine of glutamine, which is altered by H/D exchange, can affect the efficiency of the ^{1}H–^{15}N CRE effect.

In general, deuterium in a radical solution is known to be beneficial for improving the diffusion of polarization from the sites of initial electron–nucleus polarization transfer to nuclei far away from the radical center and to increase the polarization transfer efficiency from protons to heteronuclei through relaxation–prolongating effects [35–37]. While some protons in the radical solution are needed to spread the polarization in the bulk, too many or too little of them can weaken the enhancement. In NMR of biological

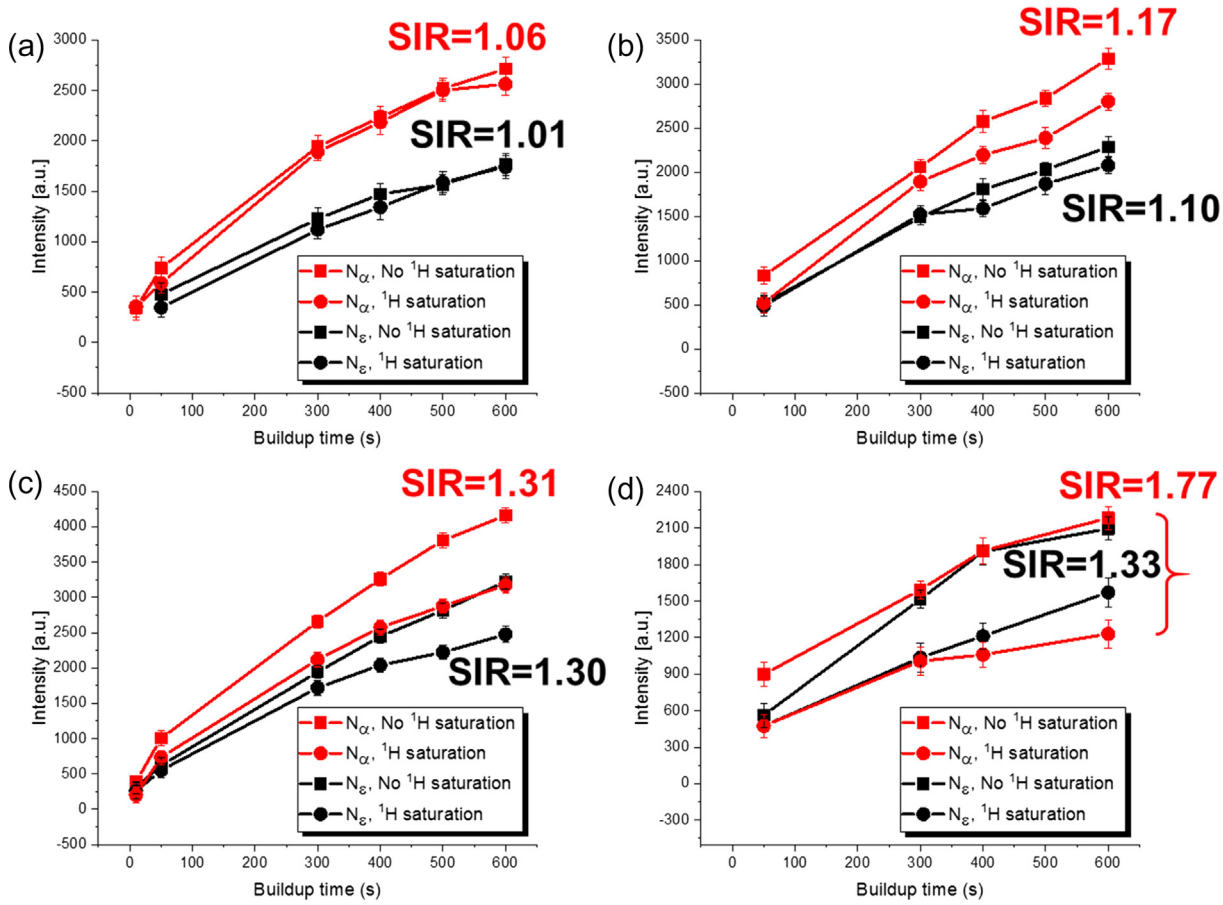

Fig. 5. (a)~(c) Polarization build-up curves for the ammonium (N_α, red) and the amide (N_ε, black) of the glutamine sample at 100 K depending on ^1H concentrations in the radical solution. (a) glycerol-d_8/D_2O/H_2O (60/30/10 vol%); (b) glycerol-d_8/H_2O (60/40 vol%); (c) glycerol/H_2O (60/40 vol%) mixture containing 10 mM AMUPol radical. Experimental peak intensities for DP and DP_{sat} experiments with MW are represented by square and circle symbols respectively. (d) Polarization build-up curves at 140 K in the radical solution composition as in (c). The signal intensity ratio depending on the presence of a ^1H saturation pulse in the polarization build-up time of 600 s is represented by SIR. (For interpretation of the references to colour in this figure legend, the reader is referred to the web version of this article.)

samples, the radical solution composition used for the spectrum shown in Fig. 5(a) has generally lead to the best performance [38]. However, when comparing the intensities of the plots in Fig. 5(a–c), the ^{15}N NMR signal intensity for glutamine increases with higher ^1H concentration. The relative concentrations of the free proton in the radical solvents have a H/D (molar/molar) ratio of 16:84, 64:36, and 100:0. We further determined the DNP enhancement factor ($\varepsilon_{15N\ CP}$) of ^{15}N CPMAS (Fig. S6, Table S1) and with this the ^1H polarization. A change in the protonation degree from 64% to 100% results in a decrease of the ^1H polarization by a factor of 0.7, while in the DP experiment the additional signal by the CRE effect increases by a factor of about 2. Therefore, under the tested experimental conditions, for glutamine the ^1H-^{15}N CRE effect modulated by the amine protons appears to be more significant for the signal enhancement than the relaxation-prolongating effect of the deuterium.

To confirm the difference in CRE by the dynamic properties of the two nitrogen groups (N_α and N_ε) in glutamine, the temperature was increased to 140 K. In Fig. 5(c) and (d), the fully protonated sample is compared at different temperatures. The rate of change of the enhancement factor for N_α is more sensitive than that of N_ε. The structure of glutamine at neutral pH contains zwitterionic forms consisting of an α-amino group (N_α) in the protonated $-NH_3^+$ form and a carboxylic acid group in the deprotonated $-COO^-$ form, and a simple amide (N_ε) side chain. As can be seen in Fig. S7, the amide (N_ε) side chain is stabilized due to the partial-double bond, resulting in slower dynamics. Therefore, the amide (N_ε) side chain, which may have a smaller change in dynamics when the temperature is increased, experiences a smaller CRE effect on the spectrum.

5. Conclusions

We have shown evidence for the CRE effect, resulting in additional positive signal enhancement for the ^{15}N NMR spectrum, by the spontaneous polarization transfer from hyperpolarized ^1H to ^{15}N during ^{15}N DP-MAS DNP. A larger CRE effect can be achieved in an aprotic solvent due to the prevention of H/D exchange between solvent and substrate, as well as a more rapid reorientation dynamics of N-functional groups caused by weaker interactions.

Similar to a previous application [24] of a specific CRE by active motion under DNP (SCREAM-DNP) through the introduction of a $^{13}CH_3$ labeled functional group as a probe into biomolecular systems, we expect that further surface signal enhancement using this effect could lead to more efficient and selective DNP-Surface enhanced NMR spectroscopy (DNP-SENS) in materials science. For example, surface structure information of nitrogen functionalized materials [39,40], which are prosperous as heterogeneous catalysis and energy materials, is critical for their further development. The surface signal can be selectively enhanced more strongly during DNP-SENS by binding molecules carrying rotatable nitrogen functional groups to the surface of the material. This would allow distinguishing clearly between surface and bulk signals due to a specific ^1H–^{15}N CRE effect.

Declaration of Competing Interest

The authors declare that they have no known competing financial interests or personal relationships that could have appeared to influence the work reported in this paper.

Acknowledgments

Financial support from the Max Planck Society and funding by the German Federal Ministry of Education and Research (BMBF project SABLE, grant 03EK3543 for a 600 MHz NMR spectrometer and BMBF MANGAN project, grant 03SF0509) and by the DFG (HE 3243/4-1) as well as access to the Jülich-Düsseldorf Biomolecular NMR Center are gratefully acknowledged. The authors thank Rüdiger-A. Eichel for fruitful discussions and his support of this project. H.P. thanks the dispatching for a doctoral degree by LG Chem.

Appendix A. Supplementary material

Supplementary data to this article can be found online at https://doi.org/10.1016/j.jmr.2020.106688.

References

[1] T. Maly, G.T. Debelouchina, V.S. Bajaj, K. Hu, C. Joo, T. Maly, G.T. Debelouchina, V.S. Bajaj, K. Hu, C. Joo, et al., Dynamic nuclear polarization at high magnetic fields, J. Chem. Phys. 2008 (128) (2008), https://doi.org/10.1063/1.2833582 052211.

[2] R. Griffin, T. Prisner, R. Hunter, P. Cruickshank, D. Bolton, P. Riedi, G. Smith, R. Bolton, A. Howes, E. Mark, Solid-state dynamic nuclear polarization at 263 GHz: spectrometer design and experimental results, Phys. Chem. Chem. Phys 12 (2010) 5850.

[3] A. Zagdoun, A.J. Rossini, M.P. Conley, W.R. Grüning, M. Schwarzwälder, M. Lelli, W.T. Franks, H. Oschkinat, C. Copéret, L. Emsley, et al., Improved dynamic nuclear polarization surface-enhanced NMR spectroscopy through controlled incorporation of deuterated functional groups, Angew. Chemie - Int. Ed. 52 (4) (2013) 1222–1225, https://doi.org/10.1002/anie.201208699.

[4] A.S. Lilly Thankamony, J.J. Wittmann, M. Kaushik, B. Corzilius, Dynamic nuclear polarization for sensitivity enhancement in modern solid-state NMR, Prog. Nucl. Magn. Reson. Spectrosc. 102–103 (2017) 120–195, https://doi.org/10.1016/j.pnmrs.2017.06.002.

[5] I.V. Sergeyev, L.A. Day, A. Goldbourt, A.E. McDermott, Chemical shifts for the unusual DNA structure in Pf1 bacteriophage from dynamic-nuclear-polarization-enhanced solid-state NMR spectroscopy, J. Am. Chem. Soc. 133 (50) (2011) 20208–20217, https://doi.org/10.1021/ja2043062.

[6] M. Renault, S. Pawsey, M.P. Bos, E.J. Koers, D. Nand, R. Tommassen-Van Boxtel, M. Rosay, J. Tommassen, W.E. Maas, M. Baldus, Solid-state NMR spectroscopy on cellular preparations enhanced by dynamic nuclear polarization, Angew. Chemie - Int. Ed. 51 (12) (2012) 2998–3001, https://doi.org/10.1002/anie.201105984.

[7] B. Uluca, T. Viennet, D. Petrović, H. Shaykhalishahi, F. Weirich, A. Gönülalan, B. Strodel, M. Etzkorn, W. Hoyer, H. Heise, DNP-enhanced MAS NMR: a tool to snapshot conformational ensembles of α-synuclein in different states, Biophys. J. 114 (7) (2018) 1614–1623, https://doi.org/10.1016/j.bpj.2018.02.011.

[8] M. Afeworki, J. Schaefer, Mechanism of DNP-enhanced polarization transfer across the interface of polycarbonate/polystyrene heterogeneous blends, Macromolecules 25 (16) (1992) 4092–4096, https://doi.org/10.1021/ma00042a007.

[9] A.J. Rossini, A. Zagdoun, M. Lelli, J. Canivet, S. Aguado, O. Ouari, P. Tordo, M. Rosay, W.E. Maas, C. Copéret, et al., Dynamic nuclear polarization enhanced solid-state NMR spectroscopy of functionalized metal-organic frameworks, Angew. Chemie - Int. Ed. 51 (1) (2012) 123–127, https://doi.org/10.1002/anie.201106030.

[10] A.J. Rossini, A. Zagdoun, M. Lelli, A. Lesage, C. Copéret, L. Emsley, Dynamic nuclear polarization surface enhanced NMR spectroscopy, Acc. Chem. Res. 46 (9) (2013) 1942–1951, https://doi.org/10.1021/ar300322x.

[11] L. Piveteau, T.C. Ong, A.J. Rossini, L. Emsley, C. Copéret, M.V. Kovalenko, Structure of colloidal quantum dots from dynamic nuclear polarization surface enhanced NMR spectroscopy, J. Am. Chem. Soc. 137 (43) (2015) 13964–13971, https://doi.org/10.1021/jacs.5b09248.

[12] Y. Geiger, H.E. Gottlieb, Ü. Akbey, H. Oschkinat, G. Goobes, Studying the conformation of a silaffin-derived pentalysine peptide embedded in bioinspired silica using solution and dynamic nuclear polarization magic-angle spinning NMR, J. Am. Chem. Soc. 138 (17) (2016) 5561–5567, https://doi.org/10.1021/jacs.5b07809.

[13] Z.J. Berkson, R.J. Messinger, K. Na, Y. Seo, R. Ryoo, B.F. Chmelka, Non-topotactic transformation of silicate nanolayers into mesostructured MFI zeolite frameworks during crystallization, Angew. Chemie - Int. Ed. 56 (19) (2017) 5164–5169, https://doi.org/10.1002/anie.201609983.

[14] Andrew G.M. Rankin, J. Trébosc, F. Pourpoint, J.-P. Amoureux, O. Lafon, Recent Developments in MAS DNP-NMR of Materials, Solid State Nucl. Magn. Reson. 101 (2019) 116–143.

[15] I.V. Sergeyev, B. Itin, R. Rogawski, L.A. Day, A.E. McDermott, Efficient assignment and NMR analysis of an intact virus using sequential side-chain correlations and DNP sensitization, Proc. Natl. Acad. Sci. U. S. A. 114 (20) (2017) 5171–5176, https://doi.org/10.1073/pnas.1701484114.

[16] M.A. Geiger, A.P. Jagtap, M. Kaushik, H. Sun, D. Stöppler, S.T. Sigurdsson, B. Corzilius, H. Oschkinat, Efficiency of water-soluble nitroxide biradicals for dynamic nuclear polarization in rotating solids at 9.4 T: BcTol-M and Cyolyl-TOTAPOL as New Polarizing Agents, Chem. - A Eur. J. 24 (51) (2018) 13485–13494, https://doi.org/10.1002/chem.201801251.

[17] M. Rosay, M. Blank, F. Engelke, Instrumentation for solid-state dynamic nuclear polarization with magic angle spinning NMR, J. Magn. Reson. 264 (2016) 88–98, https://doi.org/10.1016/j.jmr.2015.12.026.

[18] T.F. Kemp, H.R.W. Dannatt, N.S. Barrow, A. Watts, S.P. Brown, M.E. Newton, R. Dupree, Dynamic nuclear polarization enhanced NMR at 187 GHz/284 MHz using an extended interaction klystron amplifier, J. Magn. Reson. 265 (2016) 77–82, https://doi.org/10.1016/j.jmr.2016.01.021.

[19] F.J. Scott, E.P. Saliba, B.J. Albert, N. Alaniva, E.L. Sesti, C. Gao, N.C. Golota, E.J. Choi, A.P. Jagtap, J.J. Wittmann, et al., Frequency-agile gyrotron for electron decoupling and pulsed dynamic nuclear polarization, J. Magn. Reson. 289 (2018) 45–54, https://doi.org/10.1016/j.jmr.2018.02.010.

[20] M.M. Hoffmann, S. Bothe, T. Gutmann, G. Buntkowsky, Unusual local molecular motions in the solid state detected by dynamic nuclear polarization enhanced NMR spectroscopy, J. Phys. Chem. C 121 (41) (2017) 22948–22957, https://doi.org/10.1021/acs.jpcc.7b07965.

[21] V. Aladin, B. Corzilius, Methyl dynamics in amino acids modulate heteronuclear cross relaxation in the solid state under MAS DNP, Solid State Nucl. Magn. Reson. 99 (2019) 27–35.

[22] D. Daube, V. Aladin, J. Heiliger, J.J. Wittmann, D. Barthelmes, C. Bengs, H. Schwalbe, B. Corzilius, Heteronuclear cross-relaxation under solid-state dynamic nuclear polarization, J. Am. Chem. Soc. 138 (51) (2016) 16572–16575, https://doi.org/10.1021/jacs.6b08683.

[23] M.M. Hoffmann, S. Bothe, T. Gutmann, F.-F. Hartmann, M. Reggelin, G. Buntkowsky, Directly vs indirectly enhanced 13 C in dynamic nuclear polarization magic angle spinning NMR experiments of nonionic surfactant Systems, J. Phys. Chem. C acs.jpcc.6b13087 (2017), https://doi.org/10.1021/acs.jpcc.6b13087.

[24] V. Aladin, M. Vogel, R. Binder, I. Burghardt, B. Suess, B. Corzilius, Complex formation of the tetracycline-binding aptamer investigated by specific cross-relaxation under DNP, Angew. Chemie - Int. Ed. (2019) 4863–4868, https://doi.org/10.1002/anie.201811941.

[25] R. Kaiser, Use of the nuclear overhauser effect in the analysis of high-resolution nuclear magnetic resonance spectra, J. Chem. Phys. 39 (10) (1963) 2435–2442, https://doi.org/10.1063/1.1734045.

[26] J.L. White, J.F. Haw, Nuclear overhauser effect in solids, J. Am. Chem. Soc. 112 (15) (1990) 5896–5898, https://doi.org/10.1021/ja00171a049.

[27] N. Giraud, M. Blackledge, A. Böckmann, L. Emsley, The influence of Nitrogen-15 proton-driven spin diffusion on the measurement of Nitrogen-15 longitudinal relaxation times, J. Magn. Reson. 184 (1) (2007) 51–61, https://doi.org/10.1016/j.jmr.2006.09.015.

[28] E.A. Fry, S. Sengupta, V.C. Phan, S. Kuang, K.W. Zilm, CSA-enabled spin diffusion leads to MAS rate-dependent T 1′s at high field, J. Am. Chem. Soc. 133 (5) (2011) 1156–1158, https://doi.org/10.1021/ja106730p.

[29] I. Solomon, Relaxation processes in a system of two spins, Phys. Rev. 99 (1955) 559.

[30] M. Bennati, I. Tkach, M.T. Türke, Dynamic Nuclear Polarization in Liquids vol. 22 (2011) 22.

[31] D. Neuhaus, C.P.M. van Mierlo, Measurement of Heteronuclear NOE enhancements in biological macromolecules. A convenient pulse sequence for use with aqueous solutions, J. Magn. Reson. 100 (1) (1992) 221–228, https://doi.org/10.1016/0022-2364(92)90382-H.

[32] A. Zagdoun, G. Casano, O. Ouari, M. Schwarzwälder, A.J. Rossini, F. Aussenac, M. Yulikov, G. Jeschke, C. Copéret, A. Lesage, P. Tordo, L. Emsley, Large molecular weight nitroxide biradicals providing efficient dynamic nuclear polarization at temperatures up to 200 K, J. Am. Chem. Soc. 135 (34) (2013) 12790–12797, https://doi.org/10.1021/ja405813t.

[33] C. Sauvée, M. Rosay, G. Casano, F. Aussenac, R.T. Weber, O. Ouari, P. Tordo, Highly efficient, water-soluble polarizing agents for dynamic nuclear polarization at high frequency, Angew. Chem. Int. Ed. (2013) 10858–10861, https://doi.org/10.1002/anie.201304657, No. Scheme 1.

[34] V. Chevelkov, K. Faelber, A. Schrey, K. Rehbein, A. Diehl, B. Reif, Differential line broadening in MAS solid-state NMR due to dynamic interference, J. Am. Chem. Soc. 129 (33) (2007) 10195–10200, https://doi.org/10.1021/ja072024c.

[35] G.J. Gerfen, L.R. Becerra, D.A. Hall, R.G. Griffin, R.J. Temkin, D.J. Singel, High frequency (140 GHz) dynamic nuclear polarization: polarization transfer to a solute in frozen aqueous solution, J. Chem. Phys. 102 (1995) 9494–9497.

[36] K.N. Hu, H.H. Yu, T.M. Swager, R.G. Griffin, Dynamic nuclear polarization with biradicals, J. Am. Chem. Soc. 126 (35) (2004) 10844–10845, https://doi.org/10.1021/ja039749a.

[37] Ü. Akbey, H. Oschkinat, Structural biology applications of solid state MAS DNP NMR, J. Magn. Reson. 269 (2016) 213–224, https://doi.org/10.1016/j.jmr.2016.04.003.

[38] B. Corzilius Paramagnetism in Experimental Biomolecular NMR (Chapter 8. Dynamic Nuclear Polarization); Royal Society of Chemistry, 2018. https://doi.org/10.1039/9781788013291.
[39] J.W. Straten, P. Schleker, M. Krasowska, E. Veroutis, J. Granwehr, A.A. Auer, W. Hetaba, S. Becker, R. Schlögl, S. Heumann, Nitrogen-functionalized hydrothermal carbon materials by using urotropine as the nitrogen precursor, Chem. - A Eur. J. 12298–12317 (2018), https://doi.org/10.1002/chem.201800341.
[40] H. Park, P.P.M. Schleker, Z. Liu, N. Kowalew, T. Stamm, R. Schlögl, R.-A. Eichel, S. Heumann, J. Granwehr, Insights on water interaction at the interface of nitrogen functionalized hydrothermal carbons, J. Phys. Chem. C acs. jpcc.9b05323 (2019), https://doi.org/10.1021/acs.jpcc.9b05323.